NEURO

Optimising MR perfusion imaging: comparison of different software-based approaches in acute ischaemic stroke

Lars-Arne Schaafs[1,2] · David Porter[3] · Heinrich J. Audebert[4] · Jochen B. Fiebach[2] ·
Kersten Villringer[2]

Abstract

Objectives Perfusion imaging (PI) is susceptible to confounding factors such as motion artefacts as well as delay and dispersion (D/D). We evaluate the influence of different post-processing algorithms on hypoperfusion assessment in PI analysis software packages to improve the clinical accuracy of stroke PI.

Methods Fifty patients with acute ischaemic stroke underwent MRI imaging in the first 24 h after onset. Diverging approaches to motion and D/D correction were applied. The calculated MTT and CBF perfusion maps were assessed by volumetry of lesions and tested for agreement with a standard approach and with the final lesion volume (FLV) on day 6 in patients with persisting vessel occlusion.

Results MTT map lesion volumes were significantly smaller throughout the software packages with correction of motion and D/D when compared to the commonly used approach with no correction ($p = 0.001–0.022$). Volumes on CBF maps did not differ significantly ($p = 0.207–0.925$). All packages with advanced post-processing algorithms showed a high level of agreement with FLV (ICC = 0.704–0.879).

Conclusions Correction of D/D had a significant influence on estimated lesion volumes and leads to significantly smaller lesion volumes on MTT maps. This may improve patient selection.

Key Points
- *Assessment on hypoperfusion using advanced post-processing with correction for motion and D/D.*
- *CBF appears to be more robust regarding differences in post-processing.*
- *Tissue at risk is estimated more accurately by correcting software algorithms.*
- *Advanced post-processing algorithms show a higher agreement with the final lesion volume.*

Jochen B. Fiebach and Kersten Villringer contributed equally to this work.

✉ Lars-Arne Schaafs
lars-arne.schaafs@charite.de

[1] Department of Radiology, Charité-Universitätsmedizin, Hindenburgdamm 30, 12203 Berlin, Germany

[2] Academic Neuroradiology, Department of Neurology and Center for Stroke Research, Charité-Universitätsmedizin, Berlin, Germany

[3] Fraunhofer Institute for Medical Image Computing MEVIS, Bremen, Germany

[4] Department of Neurology with Experimental Neurology, Charité-Universitätsmedizin, Berlin, Germany

Abbreviations

AIF	arterial input function
CBF	cerebral blood flow
cSVD	singular value decomposition with a block-circulant matrix
D/D	delay and dispersion
FLV	final lesion volume
ICC	intraclass correlation coefficient
MTT	mean transit time
SVD	singular value decomposition
sSVD	standard truncated singular value decomposition

Introduction

Multi-parametric stroke MRI is thought to support a patient selection for thrombolysis based on the actual extent of potentially salvageable tissue at risk rather than on the mandated time window of <4.5 h [1, 2]. This concept is based on the theory of a mismatch between diffusion- (DWI) and perfusion (PI)-weighted imaging where DWI reflects the irreversibly damaged ischaemic core and PI depicts critically hypoperfused but still potentially viable tissue, with the latter being the target of a thrombolytic therapy [1–3]. Dynamic susceptibility contrast MRI (DSC-MRI) is the preferred method for performing PI in stroke [4]. There are however some shortcomings in the quantification of perfusion such as issues measuring the arterial input function (AIF) and deconvolving the concentration time curve afterwards [4–6]. The AIF is defined as the time-dependent input of contrast agent into a voxel and is derived from the measurement of signal intensity across multiple time points before, during and after the passage of the contrast agent bolus through the artery [7]. The optimal location to measure the AIF remains controversial [7, 8]. The AIF in distal arterioles reflects the actual haemodynamics but can be distorted by partial volume effects (PVEs) because of the relatively low spatial resolution of PI. Conversely, an AIF in larger arteries is thought to overcome PVE but is prone to delay and dispersion (D/D) of the bolus [5, 6, 9]. The term delay refers to the fact that a temporal delay occurs if the AIF is measured proximal to the actual entrance of the contrast agent into the tissue of interest. The delay increases even further if there are flow abnormalities caused by stenosis or collateral flow, and such abnormalities can result in a dispersion of the bolus due to a distortion of the measured concentration-time curve. Both delay and dispersion may falsify perfusion measurement if not taken into account during the process of quantification. Moreover, it is still under debate whether the AIF should be represented as a global input for the whole brain with no regard for the localised haemodynamic behaviour [7]. Another approach has been proposed using a local input function with one or multiple AIFs, each representing the blood supply to a specific small region of tissue [10]. Although it was shown that a local AIF could minimise the quantification errors by PVE and especially D/D, there is still a controversy about its effectiveness regarding the reduction of D/D-related errors when compared to the commonly used global input [11, 12]. Deconvolution is generally carried out by using a standard truncated singular value decomposition (sSVD) and describes a mathematical approach to remove the temporal spread associated with the AIF from the time-concentration curve [4]. The model of sSVD assumes that the measured AIF reflects the exact input with no D/D of the bolus and is therefore another possible source of quantification errors resulting in a significant underestimation of cerebral blood flow (CBF) [5]. Lastly, head movement decreases the diagnostic accuracy of MRI and has been shown to underestimate the

hypoperfusion volume [13]. While many solutions have been proposed to overcome quantification errors by motion artefacts and D/D, the post-processing techniques are not widely used in clinical routine. Before fully integrating these correction procedures into routine clinical practice, a detailed evaluation is required. The aim of our study is to test PI analysis software packages with advanced algorithms for correction of motion and D/D regarding the depiction of critically perfused tissue in patients with acute stroke.

Methods

Patients

According to standard department practice, all eligible patients with symptoms of an acute stroke are examined in a clinical stroke research dedicated stroke MRI system during daytime using a multiparametric sequence protocol. Patients included in this study were examined according to the aforementioned standard practice over a period of 13 months. Study inclusion criteria were: age of ≥18 years, acute DWI lesion and perfusion deficit, MRI imaging within the first 24 h after symptom onset and subsequent imaging on the 2nd and 6th days. Patients imaged outside of working hours with an inability to undergo MRI or with an acute or chronic renal failure were excluded. Written consent was obtained from all patients or legal representatives. This study is IRB approved.

MRI imaging

Imaging was performed on a 3-T MRI (Siemens Magnetom Trio, Siemens AG, Healthcare Sector, Erlangen, Germany) with a 12-channel head coil. For PI 5 ml Gadovist® (1 mmol/l Gadubutrol, Bayer Schering Pharma) followed by 20 ml saline flush was injected at a flow rate of 5 ml/s using an automatic injector (Spectris, Medrad Inc., USA). Imaging parameters for bolus tracking DSC-MRI were as follows: TR = 1390 ms; TE = 29 ms; matrix size = 128 × 128; FOV = 230 mm; slice thickness = 5 mm. Injection of Gadovist started with a 10-s delay. The sequence parameters for DWI were: TR = 6700 ms; TE = 93 ms; b = 0 s/mm^2 and 1000 s/mm^2; matrix size = 192 × 192; FOV = 230 mm; slice thickness = 2.5 mm. Parameters for time-of-flight MRA were: TR = 22 ms; TE = 3.86 ms; matrix size = 384 × 268; FOV = 200 mm; slice thickness = 0.65 mm. Sequence parameters for FLAIR were: TR = 8000 ms; TE = 100 ms; matrix size = 256 × 256; FOV = 220 mm; slice thickness = 5.0 mm.

PI post-processing

The standard software provided by the manufacturer (referred to as "Package A", Siemens AG, Healthcare Sector, Erlangen,

Germany) utilises a manual AIF selection followed by a sSVD as the deconvolution method. The AIF is used as a global input function.

A second software package (referred to as "Package B") provided by the manufacturer (Siemens AG, Healthcare Sector, Erlangen, Germany) contains a motion correction and a fully automated algorithm for AIF detection and optimisation, developed by Lorenz, Benner et al. [14]. Motion correction is realised using a rigid body transformation with interpolation. The local AIF for each voxel is obtained as the mean of multiple measured signal curves from adjacent, surrounding voxels. Deconvolution is carried out by sSVD.

The third, in-house developed software [fast light medical time series viewer (FLMTV), Peter Brunecker] uses an algorithm that optimises the selected AIF by transforming it based on a transport-diffusion theory [15, 16]. This AIF is used as a global input. Deconvolution is carried out with a block-circulant matrix SVD (cSVD) developed by Wu et al. [17]. To further evaluate the influence of motion correction and the combination of different post-processing methods, we combined the motion correction of Package B with the algorithms of FLMTV (the combination of both is referred to as "Package C"). FLMTV without a previous motion correction is referred to as "Package D".

Additionally, we tested a second motion correction algorithm called MCFLIRT developed by Jenkinson et al., which is part of the FMRIB Software Library (Oxford Centre for Functional MRI of the Brain, Oxford, UK) [18, 19]. It utilises a rigid body transformation with trilinear interpolation. Registration of motion is realised in consecutive steps with an increasing spatial resolution and increasing degree of freedom. We chose the maximum of four steps with an increasing spatial resolution up to 1 mm. Perfusion maps were calculated afterwards using FLMTV (the combination is referred to as "Package E").

The PI data sets were post-processed to calculate relative perfusion maps with the commonly used parameters CBF and MTT. We calculated maps with Packages A-C resulting in three MTT and CBF maps for each of the 50 patients. Additionally, 30 of 50 randomly chosen data sets were post-processed with Packages D and E, resulting in a total of five MTT and CBF maps for each patient. The sub-analysis with Packages D and E was introduced to better assess the impact of different corrections for D/D and for motion on estimation of hypoperfusion.

Approximate computing times are as follows: Package A, 3 min; Package B, 20 min; Package C, 25 min; Package D, 20 min; Package E, 25 min. Table 1 contains a summary of the relevant technical key points of each software package.

Image review

In case of Packages A and C-E, a manual selection of AIF in the distal MCA branches of the contralateral hemisphere as proposed by Ebinger et al. was performed and regions of interest (ROI) were manually drawn on PI images and on DWI day-1 images by a single trained reader (LAS) [8]. Final lesion volume (FLV) was employed as an outcome parameter and was determined by drawing a ROI on FLAIR day-6 images in patients with persistent vessel occlusion as proposed by Tourdias et al. [20]. Vessel status was assessed by 3D TOF-MRA day-1 and -6 images. Selection of the AIF and ROI was supervised by a senior radiologist (KV and JBF) in each single case. Lesion volumes were calculated by multiplying the quantity of marked voxels with voxel dimensions and are given in millilitres. Packages B-E were analysed retrospectively and did not affect treatment decisions. However, the trained reader was blinded to the packages and final lesion volume at the time of evaluation of the PI and DWI day-1 images.

Statistical analysis

Statistical analysis was performed using SPSS 21 (IBM, Armonk, USA). Medians and SDs of all acquired lesion volumes were calculated. The Kolmogorov-Smirnov test was used to test all continuous variables for normal distribution. Afterwards, the Mann-Whitney test was performed to test for differences between groups of non-normally distributed lesion volumes. P values < 0.05 were considered statistically significant. Additionally, agreement between each evaluated software package and the standard approach was tested by calculating the systematic mean of both methods and the 95% limits of agreement, defined as the mean $\pm$ 1.96 times the SD of the mean, as part of a Bland-Altman analysis. The intraclass correlation coefficient (ICC) was used to test the agreement among Packages B-E and the agreement between the perfusion deficit on day-1 and FLV on FLAIR day-6 images in patients with persistent vessel occlusion.

Results

Patient characteristics

Fifty patients qualified with acute DWI lesions and perfusion deficits. The median age was 74 years (range: 36-89 years) and the median time from symptom onset to MRI was 221 min (range: 48-1415 min). Seventeen patients (34%) were female. The median NIHSS score on admission was 5 (range: 0-23). All patients showed signs of an acute infarction on DWI images with a median lesion volume of 4.62 ml (range: 0.04-98.35 ml). Sixteen patients (32%) received an intravenous thrombolysis with one patient (12.5% respectively 2% of the total sample) suffering from intracranial haemorrhage. There was no significant difference in final lesion volume on day 6 between thrombolysed and non-thrombolysed patients

Table 1 Summary of relevant technical key points of each software package

Package	Developer	Motion correction	AIF	Deconvolution	Computing time
A	Siemens AG, Healthcare Sector	None	Global AIF, manually selected	sSVD	3 min
B	Siemens AG, Healthcare Sector	Rigid body transformation, fully automatic	Local AIF, automatically selected and optimised	sSVD	20 min
C	In house	Rigid body transformation, fully automatic[a]	Global AIF, manually selected, automatically optimised	cSVD	25 min
D	In house	None	Global AIF, manually selected, automatically optimised[b]	cSVD[b]	20 min
E	Jenkinson et al., FMRIB, Oxford	Rigid body transformation, fully automatic, freely selectable spatial resolution and degrees of freedom	Global AIF, manually selected, automatically optimised[b]	cSVD[b]	25 min

Computing time was measured in minutes (min)

AIF arterial input function, *sSVD* standard truncated singular value decomposition, *cSVD* singular value decomposition with a block-circulant matrix

[a] Package C utilises the motion correction of Package B

[b] Packages D and E utilize the algorithm for optimising the AIF of Package C

with persisting vessel occlusion ($p = 0.394$). On day 6, 17 patients (34%) showed a persistent vessel occlusion.

Lesion volumes

Because of technical errors one data set was excluded from the sub-analysis of Packages D and E resulting in a total of 29 patients with five MTT and CBF maps each. Table 2 shows, for each software package, the medians and SDs of the lesion volumes calculated on MTT and CBF maps as well as the median difference between both parameters. Package A computed the largest lesion volume among all patients. Lesion volume on MTT maps was significantly smaller (p values between 0.001 and 0.022) when computed by Package B-E.

On CBF maps generated by Packages B-E there was no significantly smaller lesion volume when compared to Package A ($p = 0.207$-0.925). In contrast to the optimised software packages (B-E), there was a significant difference between median lesion volumes on the MTT and CBF maps ($p = 0.002$ and $p = 0.001$ respectively) when Package A was used. Figure 1 illustrates the Bland-Altman analysis for agreement between standard post-processing with Package A and post-processing with advanced algorithms in Packages B-E. ICC tested agreement between the packages with advanced algorithms in 29 patients and Packages B-E showed a very high agreement on MTT maps (ICC: 0.818-0.917) and a high to very high agreement on CBF maps (ICC: 0.786-0.97). The highest agreement across all comparisons was between lesion

Table 2 Lesion volumes on mean transit time (MTT) and cerebral blood flow (CBF) maps as well as intra-individual difference between lesion volumes on MTT and CBF maps

	50 patients			29 out of 50 patients		
	MTT (ml)	CBF (ml)	Median difference between MTT and CBF (ml)	MTT (ml)	CBF (ml)	Median difference between MTT and CBF (ml)
Package A	68.36 (30.61–121.67)	31.14 (11.94–56.78)	26.95 ± 44.46 ($p = 0.002$)	70.46 (38.78–136)	38.94 (17.64–61.18)	35.59 ± 48.56 ($p = 0.001$)
Package B	30.35 (8.38–72.31)	27.58 (7.09–51.35)	0.93 ± 26.85 ($p = 0.759$)	41.00 (8.15–75.76)	29.62 (7.57–64.50)	−1.80 ± 25.54 ($p = 0.822$)
Package C	30.17 (13.97–73.23)	26.07 (7.16–47.81)	5.67 ± 24.51 ($p = 0.232$)	34.52 (14.4–88.11)	28.36 (7.8–67−61)	5.37 ± 25.35 ($p = 0.529$)
Package D	–	–	–	33.14 (9.02–48.34)	29.76 (9.14–49.33)	0.76 ± 16.99 ($p = 0.81$)
Package E	–	–	–	42.15 (22.08–68.82)	30.24 (10.8–49.84)	6.91 ± 24.63 ($p = 0.3$)

All volumes (in millilitres) are given as median and interquartile range in parentheses. Intraindividual difference is given as median and SD with the p value in parentheses

CBF cerebral blood flow; *MTT* mean transit time

volumes on CBF maps generated by Package B and C (ICC: 0.97). Coefficients with 95% CI for MTT and CBF are given in Table 3. Comparison between Packages C-E allowed for measuring the sole influence of a motion correction. There were no significant differences between those packages (MTT: $p = 0.240$–0.680; CBF: $p = 0.768$–0.870).

Package A showed the lowest agreement between PI lesion volume and FLV in patients with persistent vessel occlusion with ICC coefficients of 0.611 for MTT and 0.694 for CBF. Tissue at risk estimated by Packages B-E showed a higher agreement with FLV on MTT and CBF maps with the highest agreement in case of MTT maps generated by Package C (ICC: 0.879). Further coefficients with 95% CI are given in Table 4.

Discussion

Lesion volumes calculated with standard software differed significantly from results calculated with algorithms for correction of motion and D/D. There was a particular lack of agreement on MTT maps with large limits of agreement and variances of up to >200 ml and up to >100 ml for CBF maps, reflecting a substantial impact of post-processing on hypoperfusion assessment. On average, Package A computed MTT maps lesion volumes, which were approximately twice as large as both the corresponding CBF lesion volumes and the MTT lesion volumes given by Packages B-E. Our results are consistent with other studies that could demonstrate that sSVD results in a significant overestimation of hypoperfusion [4, 5, 17]. Furthermore our data suggest that MTT is more prone to D/D and overestimates lesion volume, which is also comparable to other studies [5, 21]. CBF was more robust regarding differences in PI analysis and showed high agreement across software packages. Based on our observations, CBF might be more suited to assessing mismatch. This point is also supported by other studies showing CBF includes the actual tissue at risk more precisely than MTT, which is suspected of also including surrounding areas of benign oligaemia [21, 22].

Brunecker and co-workers reported that the use of a global AIF in FLMTV might be a drawback [15]. However, our results suggest that an optimised global AIF is able to correct for D/D. This is in accordance with other studies reporting a more reliable PI analysis when carefully selecting and optimising the global AIF [8, 23]. As shown by Wu and co-workers, cSVD minimises the effects of tracer D/D [17]. Therefore, it should be considered that both the optimised global AIF and cSVD might have contributed equally towards the measured lesion volumes of FLMTV when compared to the other software packages.

Previous studies have indicated that a local AIF, as used in Package B, minimises the effects of D/D and estimates higher

CBF and lower MTT values with controversies still remaining as to whether the estimated lesion volumes reflect the actual haemodynamics [10–12]. While our results are in agreement concerning smaller lesion volumes, we assume that the use of an sSVD remains a source of quantification errors for larger lesion volumes since it is highly sensitive to D/D [4, 5]. Nevertheless, Packages B and C showed the highest agreement across all comparisons, which illustrates that both approaches are similarly effective.

By using the same algorithms for AIF and SVD in Package C and E we were able to compare two approaches to applying motion correction in PI. These software packages showed a good agreement on MTT and CBF maps with no significant differences, implying that there is a common influence on the estimated lesion volume. We could not determine substantial differences in lesion volumes in Packages C and E compared to Package D. This leads to the suggestion that motion correction does not influence PI analysis to the same degree as the optimisation of AIF and SVD. Kosior and co-workers have shown a wider influence of head motion and its correction on perfusion quantification with motion artefacts causing a significant underestimation of ischaemia [13]. Since we did not quantify head movement, a possible explanation for the comparatively small impact of motion correction might be the absence of severe head movement in our cohort. Another potential explanation is a missing effectiveness of the evaluated rigid body transformations, which is supported by Krings et al. who have shown a rigid body transformation to be effective only if head movement was below 1.5 mm in case of T2-weighted echo planar imaging sequences [24]. Moreover, it has been suggested that a trilinear interpolation as used in FSL might be inferior to other approaches because of increased image smoothing [25].

In conclusion, a PI analysis tool using a global AIF and sSVD may significantly overestimate tissue at risk when no correction is applied for D/D and such tools should be used with caution in acute stroke imaging, since it might affect the estimation of the viable ischaemic tissue [26]. Agreement between the software Packages B-E was high (ICC 0.786–0.97) throughout all comparisons. This test demonstrates that despite the two different approaches, Package B (global but optimised AIF + cSVD) and Package C (local AIF + sSVD) result in a similar net response to D/D, although there might still be some common confounding effects, which result in deviations of lesion volume estimates from the true values. Furthermore, the generally high agreement between the optimised software packages (B-E) and better agreement with FLV is an indicator of a higher reliability of corrected perfusion maps compared to the standard approach. To some extent, it is still uncertain whether Packages B-E accurately estimate the actual lesion volume since our data have solely been validated against outcome on FLAIR day-6 images but not against the gold standard of PET.
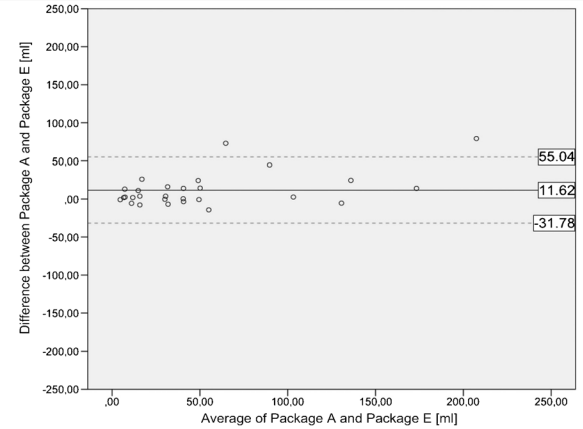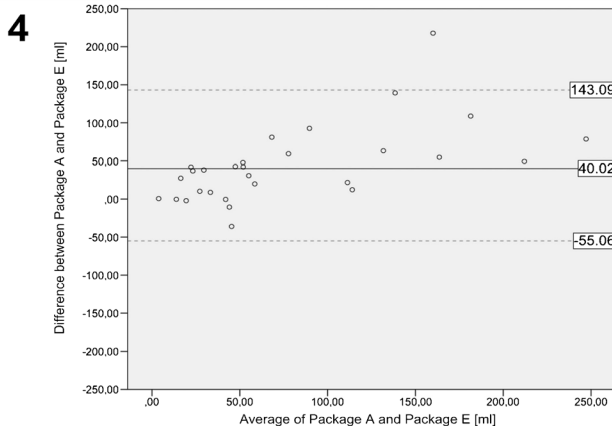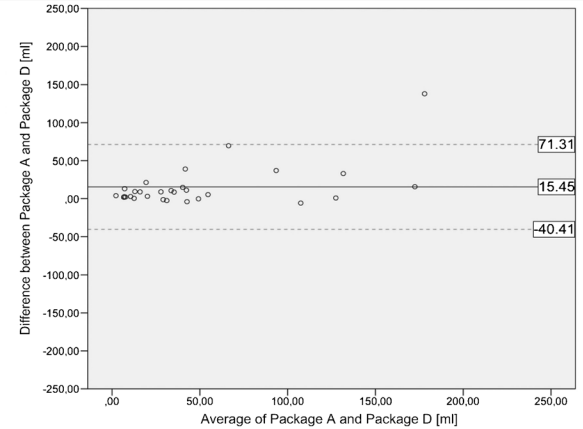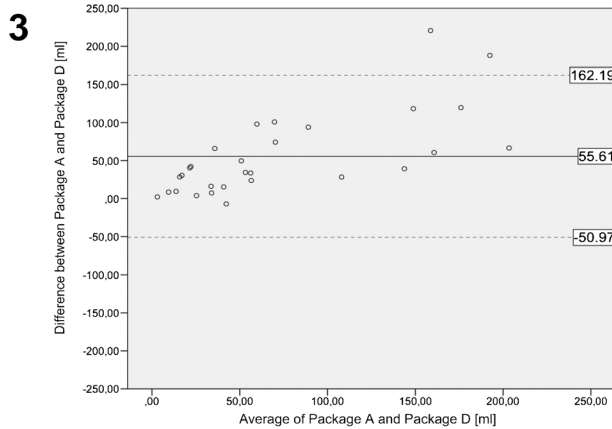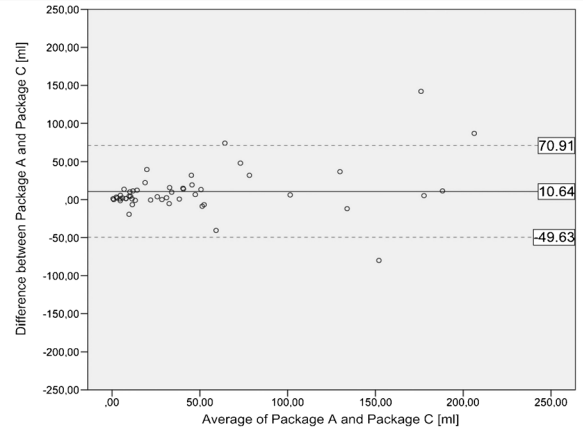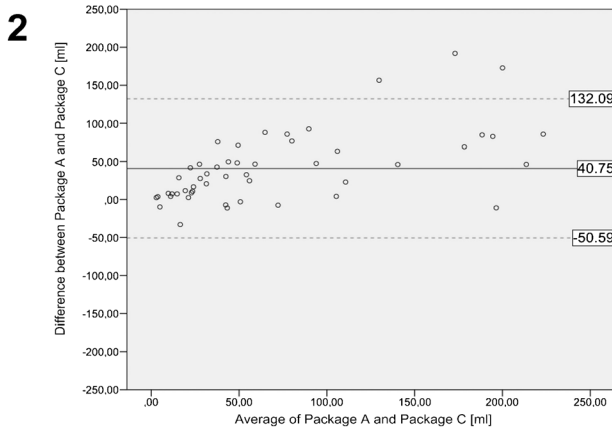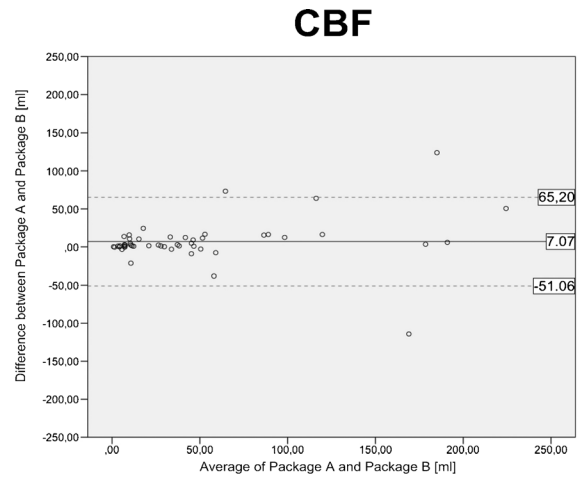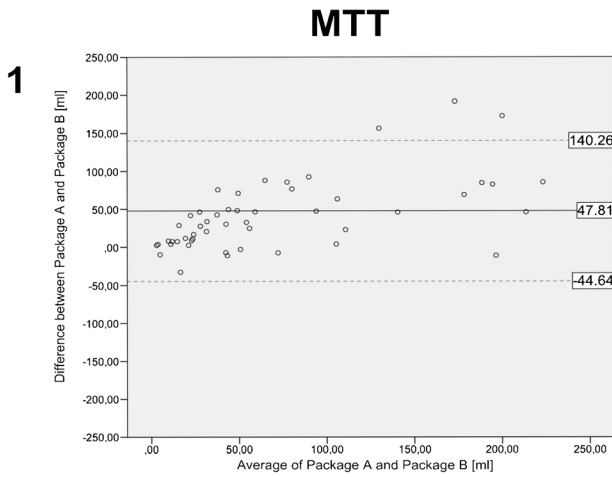
MTT　　　　　　　　CBF

◀ **Fig. 1** Bland-Altman plot including limits of agreement between Package A and each of the advanced Packages B-E. Agreement on MTT maps is shown in the *left column*, whereas agreement on CBF maps is shown in the *right column*. The abscissas show the mean values of lesion volumes measured on maps generated by both software packages. The ordinates show the difference between lesion volumes. All volumes are given in millilitres. *1* Agreement between Package A and B. *2* Agreement between Package A and C. *3* Agreement between Package A and D. *4* Agreement between Package A and E. MTT maps show limits of agreement between 182.68–213.16 ml and variances of up to >200 ml. Lesion volumes on CBF maps show limits of agreement between 86.82–120.54 ml and variances of up to >100 ml

As recent studies have pointed out, a proper post-processing of PI data in terms of a correction for D/D is essential for a reliable assessment of perfusion, especially since sSVD remains one of the most common deconvolution techniques in vendor-specific and non-proprietary software packages [27, 28]. Emphasis in our study was placed on the applicability of optimised PI imaging in acute stroke imaging. Our study provides new results suggesting that software packages are available that enable PI to be more reliable and therefore it may support the evaluation of thrombolysis. This is contrary to previous studies of Galinovic et al. who showed that similar software packages do not estimate the extent of hypoperfusion correctly [29, 30]. However, the computing times of the different software approaches remain a clear constraint. In view of the precept "time is brain", a computing time of at least 20 min is far too long when using mismatch assessment for the therapy decision and a computing time close to 5 min would be more favourable. Nevertheless, a manufacturer-provided package such as Package B with a fully automated AIF selection and robust optimisation methods appears to be most feasible in acute stroke imaging.

Table 3 Agreement between software Packages B-E on mean transit time and cerebral blood flow maps

MTT	Package C	Package D	Package E
Package B	0.901 (0.825–0.944)	0.917 (0.832–0.960)	0.818 (0.647–0.910)
Package C	–	0.885 (0.761–0.945)	0.838 (0.684–0.921)
Package D	–	–	0.828 (0.648–0.918)
CBF	Package C	Package D	Package E
Package B	0.97 (0.946–0.983)	0.8 (0.620–0.900)	0.786 (0.594–0.894)
Package C	–	0.864 (0.733–0.933)	0.84 (0.687–0.922)
Package D	–	–	0.954 (0.900–0.978)

Agreement was tested by intraclass correlation (ICC) with 95% confidence intervals given in parentheses. Results for MTT maps are shown in the upper box whereas results for CBF maps are shown in the lower box

CBF cerebral blood flow; *MTT* mean transit time

Table 4 Agreement between lesion volume on perfusion imaging day-1 images and final lesion volume on FLAIR day-6 images in 17 patients with persistent vessel occlusion

	MTT	CBF
Package A	0.611 (0.199–0.839)	0.694 (0.334–0.877)
Package B	0.777 (0.486–0.913)	0.783 (0.497–0.916)
Package C	0.879 (0.697–0.954)	0.812 (0.554–0.928)
Package D	0.773 (0.479–0.912)	0.732 (0.401–0.894)
Package E	0.765 (0.463–0.908)	0.704 (0.351–0.882)

Agreement between perfusion imaging and final lesion volume for mean transit time (MTT) (left column) and cerebral blood flow (CBF) maps (right column) was tested by intraclass correlation (ICC) with 95% confidence intervals given in parentheses

CBF cerebral blood flow; *MTT* mean transit time

There are some limitations to this study. First, the different number of analysed data sets in the case of Packages D and E may complicate comparison with the other approaches in our study. The decision to introduce these packages as an additional sub-analysis was made in a late stage of the study in order to better distinguish between the effects of motion correction and those relating to the advanced algorithms for AIF and SVD. Nevertheless, with 29 randomly chosen patients from the complete cohort of 50, we reached a sufficient number for a reliable statistical analysis. Second, a larger sample of patients having a persisting vessel occlusion would be needed to prove differences between Packages B-E regarding correlation of the perfusion deficit and FLV. As perfusion quantification depends on the selection of the appropriate AIF, the specific procedure of manual selection may have been a bias to our results, even though selection was performed systematically on the basis of a well-evaluated methodology and was performed by a highly trained reader. Although determination of FLV on FLAIR day-6 images is a recognised method to measure short-term radiological outcome, a validated method to assess collateral flow in MRI would be desirable and we believe that this could enhance the evaluation of FLV respectively prediction of tissue fate. Lastly, our study is limited to a small number of post-processing algorithms and PI parameters. Although our focus was on the evaluation of software packages with the most commonly used algorithms, other algorithms could potentially be more insensitive to quantification errors. We focused on MTT and CBF as perfusion parameters since they are used most commonly in our department and since the effects of D/D on other relevant parameters such as time to maximum are already well described [31, 32]. However, it cannot be ruled out that one of the tested algorithms works more effectively with a parameter not evaluated

in this study. Further studies should also focus on the question whether an optimised PI improves patient selection for thrombolysis. This has been recently discussed by Brown et al. who suggested that PI may support treatment decisions especially if patients present mild or minor symptoms [33].

Conclusion

Our three major findings were as follows: First, lesion volumes on MTT maps were significantly smaller when computed by an advanced PI analysis software. Therefore they may significantly influence mismatch volume assessment while CBF-based lesion volumes were comparable with all software packages. Second, correction for D/D has a wider influence on estimated lesion volumes than motion correction. Finally, a fully automated approach to computing PI maps seems optimal; however for acute stroke imaging further efforts have to be made to reduce the computing time.

References

1. Davis SM, Donnan GA, Parsons MW et al (2008) Effects of alteplase beyond 3 h after stroke in the Echoplanar Imaging Thrombolytic Evaluation Trial (EPITHET): a placebo-controlled randomised trial. Lancet Neurol 7:299–309
2. Hacke W, Furlan AJ, Al-Rawi Y et al (2009) Intravenous desmoteplase in patients with acute ischaemic stroke selected by MRI perfusion-diffusion weighted imaging or perfusion CT (DIAS-2): a prospective, randomised, double-blind, placebo-controlled study. Lancet Neurol 8:141–150
3. Hacke W, Albers G, Al-Rawi Y et al (2005) The Desmoteplase in Acute Ischemic Stroke Trial (DIAS): a phase II MRI-based 9-hour window acute stroke thrombolysis trial with intravenous desmoteplase. Stroke; J Cereb Circ 36:66–73
4. Ostergaard L, Weisskoff RM, Chesler DA, Gyldensted C, Rosen BR (1996) High resolution measurement of cerebral blood flow using intravascular tracer bolus passages. Part I: Mathematical approach and statistical analysis. Magn Reson Med: Off J Soc Magn Reson Med 36:715–725
5. Calamante F, Gadian DG, Connelly A (2000) Delay and dispersion effects in dynamic susceptibility contrast MRI: simulations using singular value decomposition. Magn Reson Med: Off J Soc Magn Reson Med 44:466–473
6. Østergaard L (2005) Principles of cerebral perfusion imaging by bolus tracking. J Magn Reson Imaging 22:710–717
7. Calamante F (2013) Arterial input function in perfusion MRI: a comprehensive review. Prog Nucl Magn Reson Spectrosc 74:1–32
8. Ebinger M, Brunecker P, Jungehulsing GJ et al (2010) Reliable perfusion maps in stroke MRI using arterial input functions derived from distal middle cerebral artery branches. Stroke; J Cereb Circ 41:95–101
9. Calamante F, Thomas DL, Pell GS, Wiersma J, Turner R (1999) Measuring cerebral blood flow using magnetic resonance imaging techniques. J Cereb Blood Flow Metab: Off J Int Soc Cereb Blood Flow Metab 19:701–735
10. Calamante F, Mørup M, Hansen LK (2004) Defining a local arterial input function for perfusion MRI using independent component analysis. Magn Reson Med: Off J Soc Magn Reson Med 52:789–797
11. Bleeker EJW, Webb AG, van Walderveen MAA, van Buchem MA, van Osch MJP (2012) Evaluation of signal formation in local arterial input function measurements of dynamic susceptibility contrast MRI. Magn Reson Med: Off J Soc Magn Reson Med 67:1324–1331
12. Willats L, Christensen S, Ma HK, Donnan GA, Connelly A, Calamante F (2011) Validating a local Arterial Input Function method for improved perfusion quantification in stroke. J Cereb Blood Flow Metab: Off J Int Soc Cereb Blood Flow Metab 31:2189–2198
13. Kosior RK, Kosior JC, Frayne R (2007) Improved dynamic susceptibility contrast (DSC)-MR perfusion estimates by motion correction. J Magn Reson Imaging 26:1167–1172
14. Lorenz C, Benner T, Lopez CJ et al (2006) Effect of using local arterial input functions on cerebral blood flow estimation. J Magn Reson Imaging 24:57–65
15. Brunecker P, Endres M, Nolte CH et al (2008) Evaluation of an AIF correction algorithm for dynamic susceptibility contrast-enhanced perfusion MRI. Magn Reson Med: Off J Soc Magn Reson Med 60:102–110
16. Brunecker P, Villringer A, Schultze J et al (2007) Correcting saturation effects of the arterial input function in dynamic susceptibility contrast-enhanced MRI: a Monte Carlo simulation. Magn Reson Imaging 25:1300–1311
17. Wu O, Ostergaard L, Weisskoff RM, Benner T, Rosen BR, Sorensen AG (2003) Tracer arrival timing-insensitive technique for estimating flow in MR perfusion-weighted imaging using singular value decomposition with a block-circulant deconvolution matrix. Magn Reson Med: Off J Soc Magn Reson Med 50:164–174
18. Jenkinson M, Smith S (2001) A global optimisation method for robust affine registration of brain images. Med Image Anal 5:143–156
19. Jenkinson M, Bannister P, Brady M, Smith S (2002) Improved optimization for the robust and accurate linear registration and motion correction of brain images. NeuroImage 17:825–841
20. Tourdias T, Renou P, Sibon I et al (2011) Final cerebral infarct volume is predictable by MR imaging at 1 week. AJNR Am J Neuroradiol 32:352–358
21. Parsons MW, Yang Q, Barber PA et al (2001) Perfusion magnetic resonance imaging maps in hyperacute stroke: relative cerebral blood flow most accurately identifies tissue destined to infarct. Stroke; J Cereb Circ 32:1581–1587
22. Zaro-Weber O, Moeller-Hartmann W, Heiss WD, Sobesky J (2010) MRI perfusion maps in acute stroke validated with 15O-water positron emission tomography. Stroke; J Cereb Circ 41:443–449
23. van Osch MJ, Vonken EJ, Viergever MA, van der Grond J, Bakker CJ (2003) Measuring the arterial input function with gradient echo sequences. Magn Reson Med: Off J Soc Magn Reson Med 49:1067–1076
24. Krings T, Reinges MH, Erberich S et al (2001) Functional MRI for presurgical planning: problems, artefacts, and solution strategies. J Neurol Neurosurg Psychiatry 70:749–760

25. Oakes TR, Johnstone T, Ores Walsh KS et al (2005) Comparison of fMRI motion correction software tools. NeuroImage 28:529–543

26. Sorensen AG, Copen WA, Ostergaard L et al (1999) Hyperacute stroke: simultaneous measurement of relative cerebral blood volume, relative cerebral blood flow, and mean tissue transit time. Radiology 210:519–527

27. Zaro-Weber O, Livne M, Martin SZ et al (2015) Comparison of the 2 Most Popular Deconvolution Techniques for the Detection of Penumbral Flow in Acute Stroke. Stroke; J Cereb Circ 46:2795–2799

28. Meijs M, Christensen S, Lansberg MG, Albers GW, Calamante F (2015) Analysis of perfusion MRI in stroke: To deconvolve, or not to deconvolve. Magn Reson Med: Off J Soc Magn Reson Med. doi: 10.1002/mrm.26024

29. Galinovic I, Brunecker P, Ostwaldt AC, Soemmer C, Hotter B, Fiebach JB (2011) Fully automated postprocessing carries a risk of substantial overestimation of perfusion deficits in acute stroke magnetic resonance imaging. Cerebrovasc Dis 31:408–413, **Basel, Switzerland**

30. Galinovic I, Ostwaldt A-C, Soemmer C et al (2011) Search for a map and threshold in perfusion MRI to accurately predict tissue fate: a protocol for assessing lesion growth in patients with persistent vessel occlusion. Cerebrovasc Dis 32:186–193, **Basel, Switzerland**

31. Calamante F, Christensen S, Desmond PM, Østergaard L, Davis SM, Connelly A (2010) The physiological significance of the time-to-maximum (Tmax) parameter in perfusion MRI. Stroke; J Cereb Circ 41:1169–1174

32. Kudo K, Sasaki M, Østergaard L et al (2011) Susceptibility of Tmax to tracer delay on perfusion analysis: quantitative evaluation of various deconvolution algorithms using digital phantoms. J Cereb Blood Flow Metab: Off J Int Soc Cereb Blood Flow Metab 31:908–912

33. Brown TA, Luby M, Shah J, Giannakidis D, Latour LL (2015) Magnetic resonance imaging in acute ischemic stroke patients with mild symptoms: an opportunity to standardize intravenous thrombolysis. J Stroke Cerebrovasc Dis 24:1832–1840